

Research Article

Experimental Study on Early-Age Crack of Mass Concrete under the Controlled Temperature History

Nannan Shi,¹ Jianshu Ouyang,¹ Runxiao Zhang,² and Dahai Huang¹

¹ Department of Civil Engineering, Beihang University, Beijing 100191, China

² Department of Civil Engineering, University of Toronto, Toronto, ON, Canada M5S 2E8

Correspondence should be addressed to Dahai Huang; huangdh@mail.tsinghua.edu.cn

Received 8 February 2014; Revised 6 May 2014; Accepted 13 May 2014; Published 15 July 2014

Academic Editor: Jun Liu

Copyright © 2014 Nannan Shi et al. This is an open access article distributed under the Creative Commons Attribution License, which permits unrestricted use, distribution, and reproduction in any medium, provided the original work is properly cited.

Thermal deformation under restrained conditions often leads to early-age cracking and durability problems in mass concrete structures. It is crucial to monitor accurately the evolution of temperature and thermal stresses. In this paper, experimental studies using temperature stress testing machine (TSTM) are carried out to monitor the generated thermal cracking in mass concrete. Firstly, components and working principle of TSTM were introduced. Cracking temperatures and stress reserves are selected as the main cracking evaluation indicators of TSTM. Furthermore, effects of temperature controlling measures on concrete cracking were quantitatively studied, which consider the concrete placing temperature (before cooling) and cooling rates (after cooling). Moreover, the influence of reinforcement on early-age cracking has been quantitatively analyzed using the TSTM. The experimental results indicate that the crack probability of reinforced concrete (RC) is overestimated. Theoretical calculations proved that the internal stress can transfer from concrete to reinforcement due to creep effect. Finally, the experimental results indicate that the reinforcement can improve the crack resistance of concrete by nearly 30% in the TSTM tests, and the ultimate tensile strain of RC is approximately 105% higher than that of plain concrete with the same mix proportions.

1. Introduction

Mass concrete structures are often constructed in hydraulic engineering, in which thermal stresses arise due to the cement hydration. The mass concrete, such as columns, beam, lock, pier, or dam, requires special measures of coping with the generation of thermal stress according to the ACI-116 [1]. Thermal stresses may induce early-age crack, structural damages, and further degrade structural serviceability, water tightness, and durability [2]. Only about twenty percent of cracks in mass concrete are induced by the external load, while the others are mainly caused by restrained deformation such as thermal deformation, shrinkage, and inhomogeneous deformation [2]. In addition, some massive reinforced concrete (RC) structures, such as concrete piers, walls, columns, and foundations for large structures, are much smaller than a typical concrete dam. If they are made of high performance concrete, the thermal cracking can be as serious as dams. Moreover, in the massive RC structures, the roles of reinforcement bars are limiting crack widths [3, 4].

Certain measures are used to control the temperature rising in mass concrete structures, such as the concrete placing temperature controlling (before cooling) and cooling pipes installment (after cooling). The precooling of concrete decreasing the maximum temperature of concrete was firstly employed during the Norfolk Dam construction by the corps of engineers in the early 1940s. According to the ACI-207, one of the most important measures of the thermal cracking avoidance is concrete placing temperature controlling [5]. The first major application of postcooling in mass concrete was in the Hoover Dam construction in the early 1930s [6]. The cooling measure was achieved by circulating cool water through pipes embedded in the concrete. According to the recommended practice of ACI-207, it is important to make the temperature drop as slowly as possible to allow the stress relaxation. Under the condition of slow cooling, concrete can undergo a 20°C temperature drop without cracking. Moreover, precooling and postcooling measures were applied in the construction of several dams, such as notably Glen Canyon Dam, Libby Dam, and Dworshak

TABLE 1: Tests parameters and results.

Cases	Factors	Tests	Values
Case 1	Cooling rate	1	0.33°C/h
		2	0.21°C/h
Case 2	Placing temperature	1	25.72°C
		3	20.53°C
Case 3	Reinforcement	3	Without
		4	With

Dam. It is shown that the temperature control is effective in the above projects [6]. In China, Zhu firstly introduced the application of embedded cooling pipes in 1955 [7]. In recent years, numerical simulations of thermal stresses are studied in mass concrete structures [8–10]. In the past decades, many literatures on temperature control of mass concrete are based on simulation analysis [11–17]. However, laboratory model experiments for quantitative evaluation of temperature control measures were rarely conducted.

In the previous studies, the reinforcement effects were always ignored before concrete crack in the numerical simulation. Pan indicated that the reinforcement did not have any effect before cracking especially under thermal load [18]. However, a massive RC project showed that no crack was found during the construction when the maximum thermal stress exceeded concrete tensile strength evidently [19]. Moreover, a “thermal active restrained shrinkage ring test” further shows that the reinforcement bars can postpone cracking before concrete cracks [20]. However, the study [20] has some limitations: the uncontrolled restraint degree and the smaller specimen dimension, without the measurement of reinforcement deformation.

In this paper, a series of tests based on TSTM were carried out with different concrete placing temperatures and cooling rates. Moreover, the effects of precooling and postcooling measures on concrete cracking have been quantitatively studied. RC specimens were tested based on TSTM to verify the effect of reinforcement, and the effects of reinforcement on concrete cracking were quantitatively studied. More accurate measurement specimen deformation can be achieved by installing the noncontact laser displacement sensor, and clearer effects of reinforcement on thermal cracking can be obtained by measuring the deformations of reinforcement bars.

2. Experimental Procedure

In engineering practice, three common measures are utilized to reduce thermal cracking in mass concrete: precooling, postcooling, and reinforcement configuration. To quantitatively analyze the effects of these measures, three cases are carried out (Table 1). In Case 1, two different cooling rates (0.33°C/h and 0.21°C/h) are adopted in the cooling stage of TSTM tests. In Case 2, plain concrete specimens with two different placing temperatures (25.72°C and 20.53°C) are tested using TSTM. In Case 3, plain concrete and RC with the same mix proportion are tested to consider the reinforcement

effects on the stress development and the cracking behavior. Moreover, the detailed test conditions are shown in Table 1.

The four tests in Table 1 were performed on a mass concrete with mixture proportions given in Table 2. Specimens are plain concrete in Tests 1, 2, and 3, and specimen of Test 4 is reinforcement concrete with four 12 mm diameter reinforcement bars.

2.1. Experimental Device-TSTM. The shape and dimension of the TSTM specimen are shown in Table 3. Total length of the specimen is about 2 m, and the 1.5 m central part of the specimen (red part of the specimen in Table 3) has a cross-section of 0.15 m × 0.15 m. In this paper, the measuring distance of central part maintains constant (1.5 m) throughout the test process since all TSTM-experiments are fully restrained. The dimension of the specimen should be illustrated graphically in the figure, other than described in text.

TSTM (Figure 1) is a closed-looped uniaxial restrained testing device which has four main functions: the measurement of load, the measurement and control of temperature, the measurement and control of deformation, and the measurement of reinforcement stain. For the concrete specimen, one of the cross-heads is restrained by the steel claw and the other is controlled by a stepper motor according to the specimen deformation. The load on the specimen is monitored by a load cell with accuracy of 1 N placed at the adjustable cross-head.

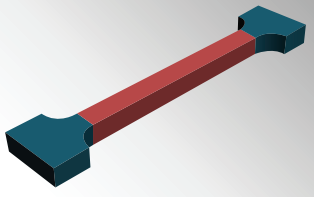
2.1.1. Measurement and Control of Temperature. The evolution of the temperature is monitored using three thermocouples placed in the central part of concrete specimen (Figure 2). The average value of the three temperature values can be calculated and recorded by the computer. Besides, “temperature control system of TSTM” is adopted to control the specimen temperature, which is composed of temperature controlled mould (test mould), pump, circulating pipes, and temperature control box (Figure 3(b)). In detail, the test mould is made of four different materials (Figure 3(a)), and the inner surface is covered with Teflon coating to minimize friction between specimen and test mould. The temperature control is ensured by the test mould through which a liquid (mixture of glycol and water) is circulating. The test mould has an outlet and inlet connecting with the “circulating pipes.” The circulatory liquid can be heated or cooled by the temperature control system according to the computer command, and then it can be pumped to the test mould which surrounded the concrete specimen (Figure 3(b)).

2.1.2. Measurement and Control of Specimen Deformation. The measured deformation of the specimen consists of thermal deformation, elastic deformation, autogenous volume deformation, and creep. The deformations of specimens are monitored by laser displacement sensors (sensor type: Omron Z4 M-W with accuracy of 0.1 μm) with invar bars that are keeping a distance of 1.5 m at the initial place (Figure 2). As the invar has a very low coefficient of thermal dilation, the length changes of the invar bars since that temperature

TABLE 2: Mixture proportions of concrete (kg/m³).

Components	Cement	Fly ash	Sand	Gravel	Total water	Water reducer	Air entraining
Mass	255	85	748	1133	146	4.074	0.068

TABLE 3: Dimension of the specimen in the TSTM (m).

Length of the span	1.5	
Width of the span	0.15	
Radius of curvature	0.75	
Width of head	0.45	
Length of head	0.15	

fluctuation can be negligible. When the deformation in the central part of the specimen exceeds the threshold ($1\mu\text{m}$), the stepper motor will pull/push the specimen back to its initial position. The load values are recorded by the computer in the whole experimental process. During the experiment, four parameters are automatically recorded: the concrete temperature values, the load values applied to the specimen, deformations of specimens, and the moving cross-head displacements.

2.1.3. Measurement of Reinforcement Deformation. To investigate the effect of reinforcement on cracking, the strain values of reinforcement bars are measured by the improved TSTM. Strain gauges are adopted to measure the deformation of reinforcement (Figure 4(a)). Two notches are milled along the longitudinal direction of the reinforcement to maintain good bond properties between gauges and reinforcement bars, in which strain gauges and the connecting cables are placed. One gauge measures the deformation in longitudinal direction and the other measures in transverse direction (Figure 4(b)), which can eliminate the thermal influences. Moreover, two of these combined gauges were placed opposite each other in one cross-section, which can correct the effect of the reinforcement bending [21].

2.2. Experimental Procedure

2.2.1. Tests with Different Temperature Histories. Firstly, fresh concrete was cast in the test mould of TSTM, and a layer of plastic sheet was covered on the surface of concrete to maintain constant humidity. Subsequently, temperature sensors and laser displacement sensors were installed (Figure 2). When TSTM starts, the specimen will be in adiabatic condition during the temperature rise stage until the temperature reaches the maximum value (temperature rise stage). In the subsequent stage, the maximum temperature will be maintained for 48 hours (constant temperature stage) to ensure enough concrete strength. Then the concrete will begin to cool with different cooling rates until crack appears (cooling stage).

2.2.2. Test of Reinforced Concrete. After reinforcement bars were assembled, strain gauges were fixed in reinforcement

TABLE 4: Results and crack indicators of TSTM.

Cases	Tests	Age/hour	σ_{rt} /MPa	σ_{cr} /MPa	$S/\%$	$T_{cr}/^\circ\text{C}$
Case 1	1	162	2.51	2.56	1.95	26.11
	2	258	1.91	2.75	30.55	17.29
Case 2	1	162	2.51	2.56	1.95	26.11
	3	135	1.57	2.35	33.19	12.21
Case 3	3	135	1.57	2.35	33.19	12.21
	4	243	1.38	3.36	58.93	-9.24

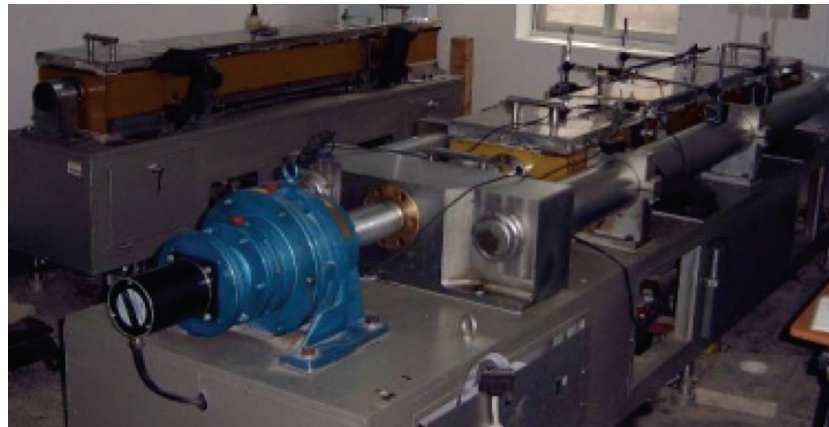
(as shown in Figure 4(a)). The same as plain concrete tests, the TSTM test of RC also has three stages: temperature rise stage, constant temperature stage, and cooling stage. Finally, the device will automatically stop when the specimen stress decrease exceeds a threshold value (1MPa) in one minute. Moreover, splitting tensile tests were carried out to verify the TSTM results. The splitting tensile tests performed at a constant temperature, different from the TSTM temperature history, can be expressed in equivalent age which is calculated by the activation energy theory. All of the stress differences between the TSTM tests and the corresponding splitting tensile tests are no more than 20%.

3. Results and Discussion

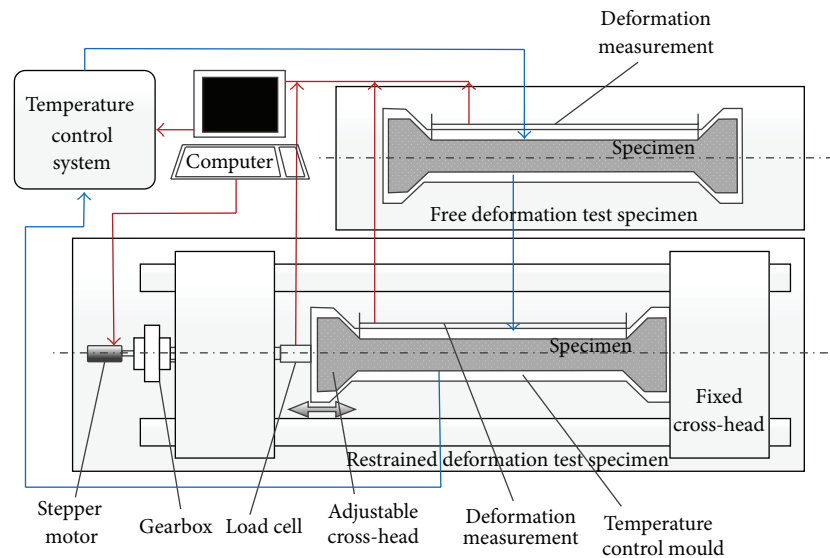
In this paper, crack resistance represents the ability of concrete to prevent cracking, and therefore enhancing the crack resistance can postpone the moment of concrete cracking. Moreover, cracking temperatures and stress reserves were chosen as the evaluation indicators of the concrete crack resistance [22]. Lower cracking temperature or higher stress reserves mean lower probability of cracking (better crack resistance). In Table 4, parameters σ_{rt} , σ_{cr} , S , and T_{cr} denote stress at room temperature, cracking stress, stress reserves, and cracking temperature, respectively. Cracking temperature and cracking stress denote the temperature and stress when concrete is cracking in TSTM test. Stress reserve represents the crack resistance capability when the temperature drops to room temperature in the cooling stage. Moreover, the stress reserve can be calculated using the following equation:

$$S = \frac{(\sigma_{cr} - \sigma_{rt})}{\sigma_{cr}} \times 100\%. \quad (1)$$

3.1. Case 1: Effects of Cooling Rates on Concrete Cracking. In Case 1, two tests (Test 1 and Test 2) are carried out with different cooling rates (0.33°C/h and 0.21°C/h) in the cooling stage. In Figure 5(a), the cracking temperature of Test 2 is 8.82°C lower than Test 1. In Table 4, the crack reserve of Test 1 is only 1.95%, which is far less than that of Test 2 (30.55%). Both of the crack indicators prove that the specimen in Test 2



(a)



(b)

FIGURE 1: Details of the experimental setup. (a) Photograph of temperature stress testing machine. (b) Schematic diagram for TSTM.

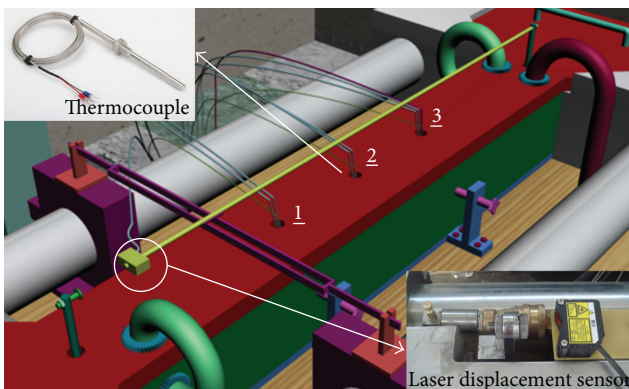


FIGURE 2: Laser displacement sensor and thermocouples.

with the lower cooling rates has better crack resistance ability than that of Test 1.

Compared with Specimen 1 (Test 1), the tensile strength of Specimen 2 (Test 2) is higher due to its higher maturity degree

of concrete (shown in Figure 5(a)), and its stress variation rate is lower that is helpful for anticrack in the early-age (seen in Figure 5(b)).

In Table 4, the age of Test 2 (258 hours) is longer than that of Test 1 (162 hours), therefore, Specimen 2 has sufficient time to redistribute the internal stress and reduce the stress concentration. In a word, the lower cooling rate can delay the concrete cracking.

3.2. Case 2: Effects of Placing Temperatures on Concrete Cracking. Higher concrete placing temperature induces higher speed of cement hydration [23]. In mass concrete, each 6°C reduction of the placing temperature below the average air temperature will result in a lowering by about 3°C of the maximum temperature of concrete [6].

Compared with Test 3, the concrete placing temperature and the adiabatic temperature rise of Test 1 are 5.2°C and 3.7°C higher, respectively (Figure 6(a)), which is consistent with the opinion of Mehta and Monteiro [6]. The higher adiabatic

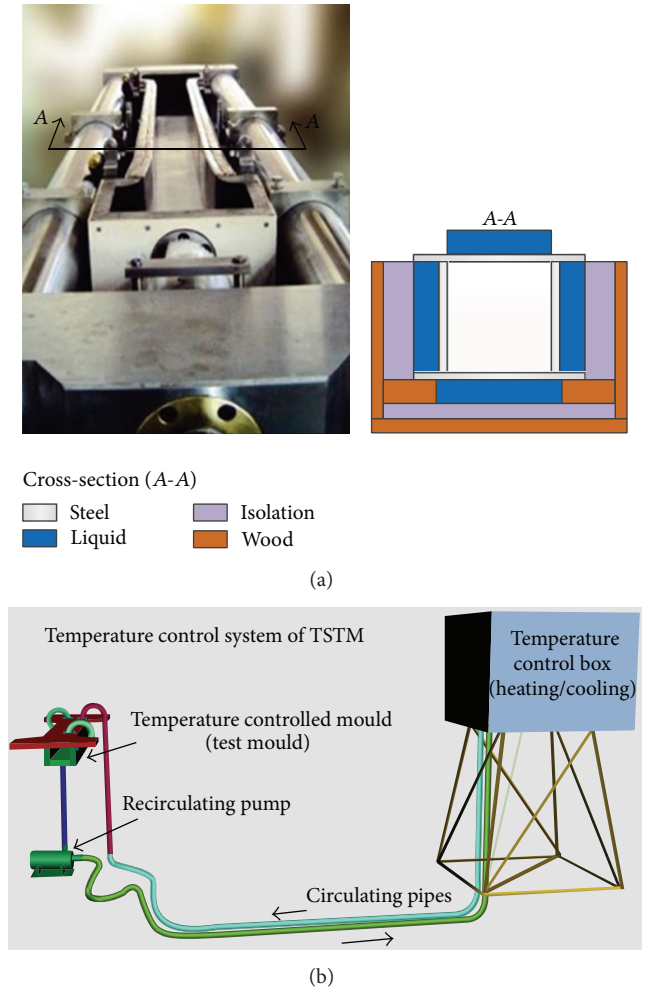


FIGURE 3: Temperature control system of TSTM. (a) Cross-section of the test mould. (b) Components of temperature control.

temperature rise of concrete causes larger thermal stress gradient, which enhances the probability of the cracking.

In Table 4, cracking temperature of Test 3 is 13.9°C (26.11°C–12.21°C) lower than that of Test 1, and the stress reserve of Test 3 is about 31.24% (33.19%–1.95%) higher than that of Test 1. Therefore, both of the crack indicators indicate that the probability of the cracking of Specimen 3 is lower. Although the cracking stress of Specimen 3 is smaller than that of the Specimen 1 (Figure 6(b)), the cracking stress cannot be considered as a reasonable indicator of cracking evaluation in the TSTM tests [24], which is less important than the above indicators (cracking temperature and stress reserve). Consequently, lower concrete placing temperature could reduce the probability of cracking.

3.3. Case 3. Effect of Reinforcement on Concrete Cracking.

In the previous studies, the reinforcement is employed to limit the crack width, but the effect of reinforcement has been neglected before concrete crack. However, the experimental results show that the reinforcement plays an obvious role on the concrete stress development (Figure 7(a) and Figure 7(b)).

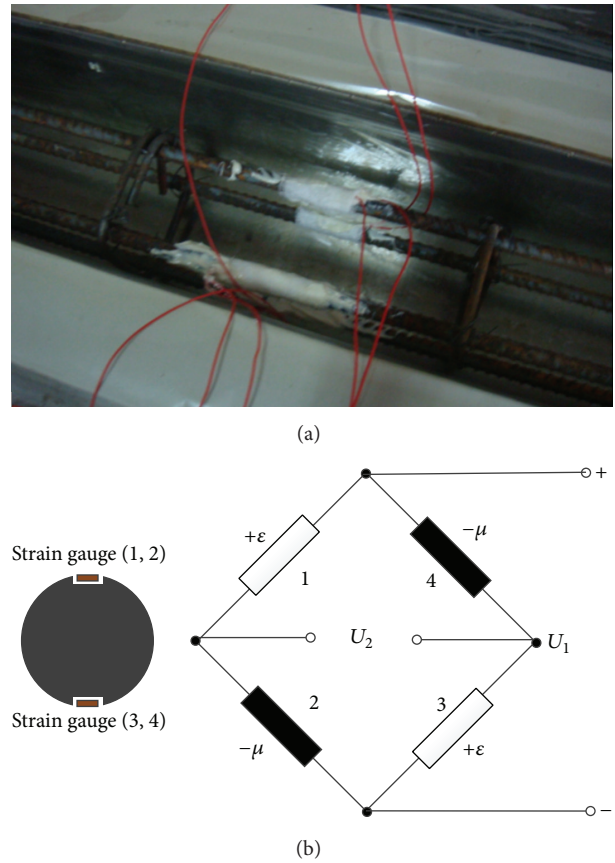


FIGURE 4: Strain gauges position of reinforcement bars in Test 4. (a) Photo of strain gauges. (b) Whole bridge formed of strain gauges.

In Table 4, the cracking temperature of RC specimen is about 21°C lower than that of plain concrete. The crack does not appear until the temperature drops to -9.24°C in Test 4, which shows that the RC specimen can resist larger temperature gradient. In addition, the stress reserve of RC (58.93%) is higher than that of plain concrete (33.19%). Therefore, RC specimen has a lower probability of cracking than that of the plain concrete.

In Figures 7(c) and 7(b), the difference of cracking stress between RC and plain concrete is about 1.01 MPa (29.76% of maximum tension stress in Test 4), and the maximum tension stress of reinforcement is 0.96 MPa (28.57% of maximum tension stress in Test 4). Consequently, reinforcement can increase the maximum tensile strength of RC specimen by nearly 30% in this experiment.

Therefore, the advantages of the reinforcement can be summarized as follows. The moment of cracking was delayed about 108 hours, the stress reserve was improved by 25.74%, and the cracking temperature was declined by 21.45°C (in the experimental conditions).

To verify the reinforcement effect on cracking under long-term load, a typical axial tension specimen was calculated, and the load on the specimen is assumed as constant to simplify the TSTM Test 4.

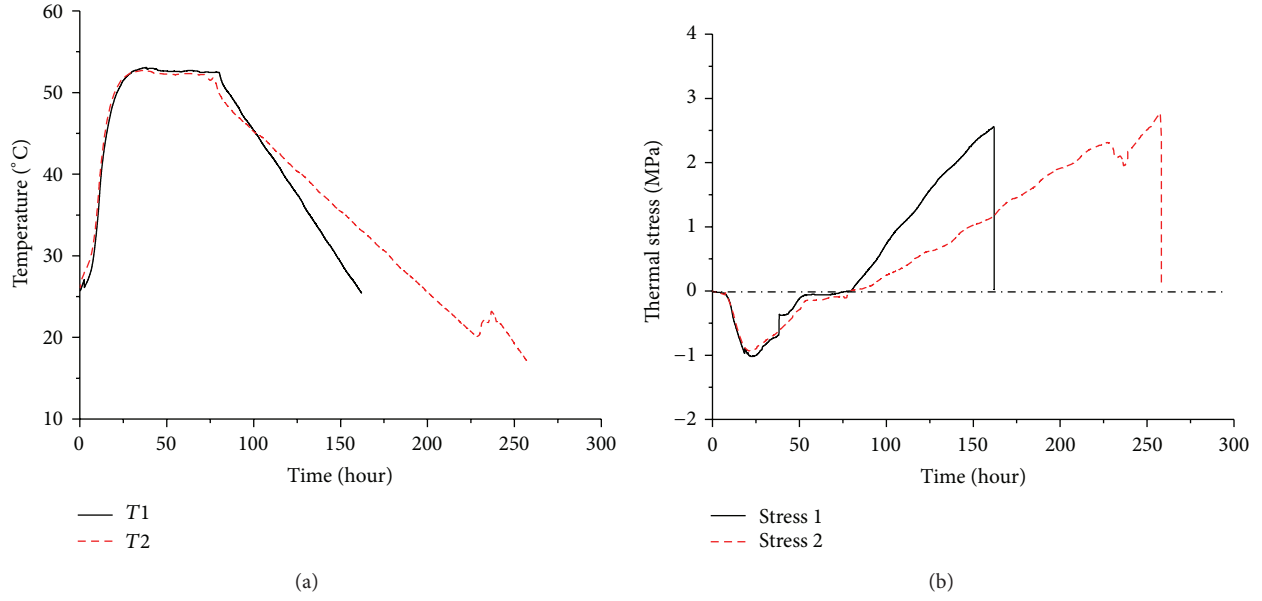


FIGURE 5: (a) Temperature curves for different cooling rates. (b) Stress curves for different cooling rates.

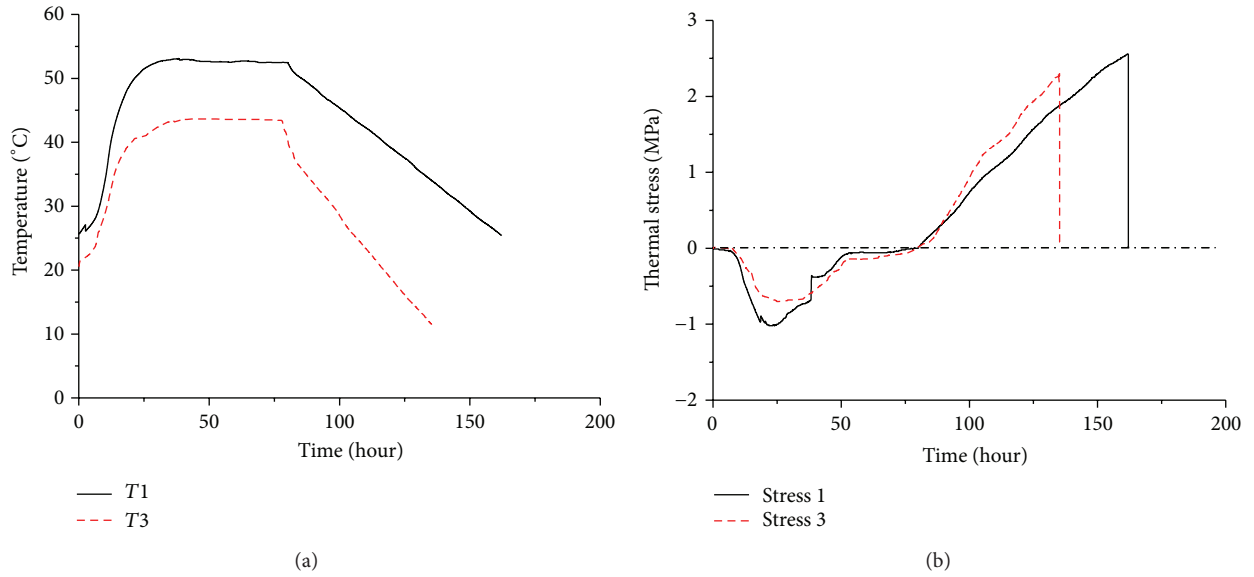


FIGURE 6: (a) Different concrete placing temperatures. (b) Stress curves under different concrete placing temperature.

Primarily, four basic assumptions are introduced: (i) there is no slip between reinforcement and concrete before cracking; (ii) specimen satisfies the plane cross-section assumption; (iii) concrete is homogeneous material and isotropic, and reinforcement is always elastic without creep; (iv) concrete satisfies the linear creep assumption and superposition principle [25].

The concrete grade is C25 with a tensile strength of 1.78 MPa ($f_{ct} = 1.78$ MPa), and its cross-section dimension is $A_0 = 150 \times 15$ mm² with four reinforcement bars (as shown in Figure 8). Besides, the rebar diameter and reinforcement ratio are 12 mm and 2%, respectively ($d = 12$ mm $\rho_s = 0.02$).

At the initial time t_0 , the mechanical equilibrium equation, concrete stress, and reinforcement stress can be expressed as

$$N(t_0) = N_c(t_0) + N_s(t_0), \quad (2)$$

$$\sigma_c(t_0) = \frac{N_c(t_0)}{A_0(1 - \rho_s)}, \quad (3)$$

$$\sigma_s(t_0) = \frac{N_s(t_0)}{A_0\rho_s}, \quad (4)$$

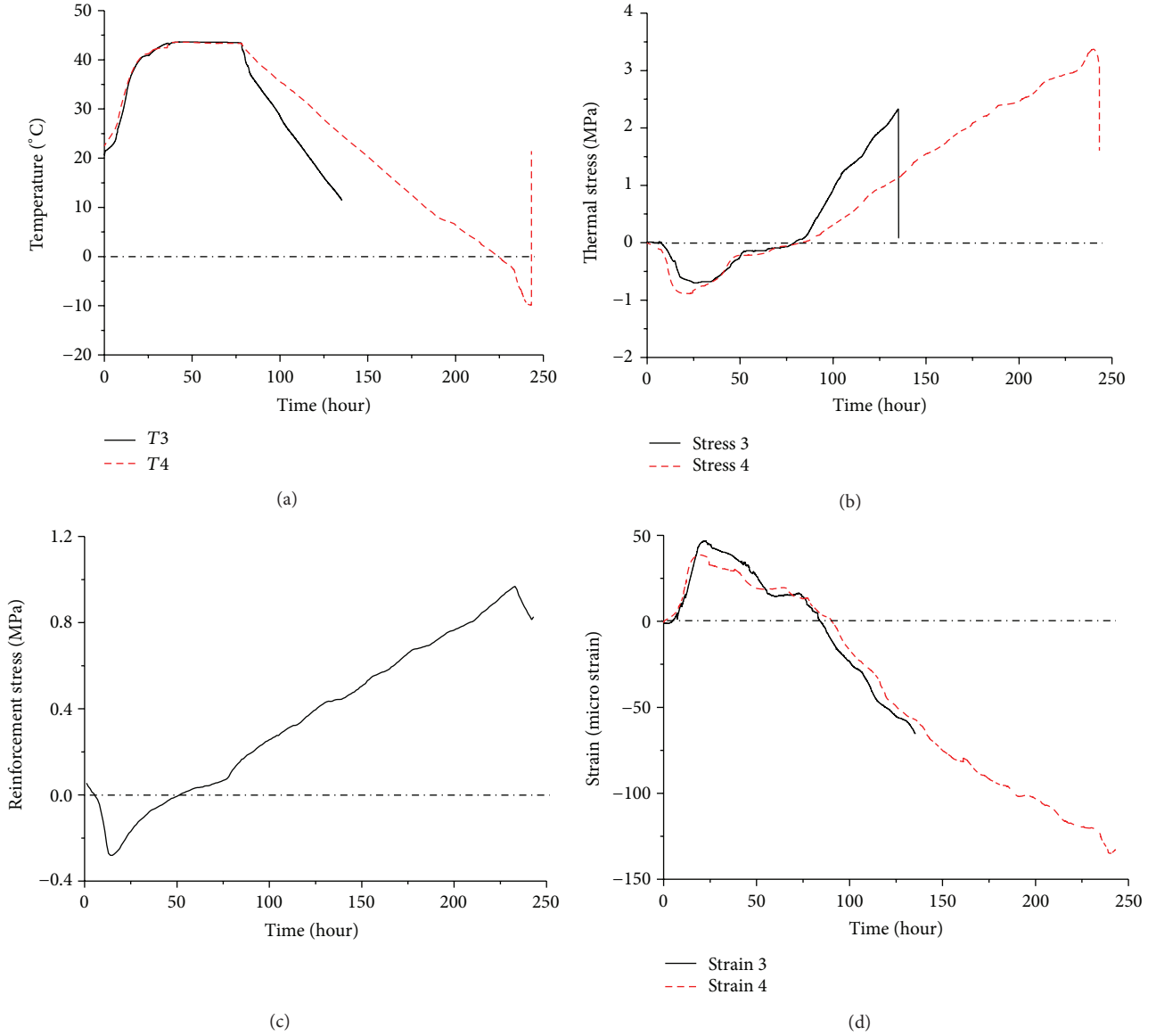


FIGURE 7: (a) Temperature curves of Tests 3 and 4; (b) stress curves of Tests 3 and 4; (c) reinforcement stress of Test 4; (d) comparison of tension strains between plain and reinforced concrete.

where N , N_c , and N_s represent the total load, the load acts on concrete, and the load acts on reinforcement, respectively; σ_c and σ_s denote stress of concrete and stress of reinforcement.

Substituting (3) and (4) into (2), $N(t_0)$ can be rewritten as

$$N(t_0) = \sigma_c(t_0) A_0 (1 - \rho_s) + \sigma_s(t_0) A_0 \rho_s. \quad (5)$$

The constitutive relations of concrete and steel bars can be expressed as

$$\begin{aligned} \varepsilon_c(t_0) &= \frac{\sigma_c(t_0)}{E_c(t_0)}, \\ \varepsilon_s(t_0) &= \frac{\sigma_s(t_0)}{E_s(t_0)}, \end{aligned} \quad (6)$$

where ε_c and ε_s are the strain of concrete and the strain of reinforcement and E_c and E_s represent the elasticity modulus of the concrete and reinforcement.

The strains of concrete and steel bars were assumed to be the same:

$$\varepsilon_c(t_0) = \varepsilon_s(t_0). \quad (7)$$

The initial stress distribution can be obtained from (5) to (7), which is expressed as

$$\begin{aligned} \sigma_c(t_0) &= \frac{N(t_0)}{A_0 (1 + (m_e(t_0) - 1) \rho_s)}, \\ \sigma_s(t_0) &= \frac{m_e(t_0) N(t_0)}{A_0 (1 + (m_e(t_0) - 1) \rho_s)}, \end{aligned} \quad (8)$$

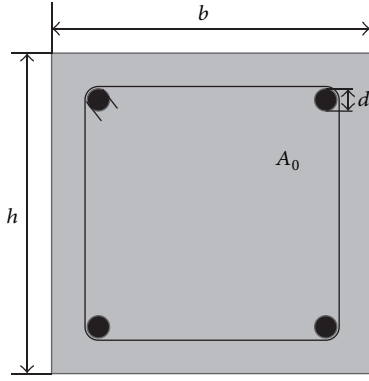


FIGURE 8: Cross-section of specimen.

where $m_e(t_0) = E_s(t_0)/E_c(t_0)$ is the ratio of reinforcement and concrete elastic modulus at time t_0 .

The “plane cross-section assumption” is still available in the long-time load, and the mechanical equilibrium equation and physical equations can be expressed as

$$\sum_{i=1}^j \Delta\sigma_s(t_i) A_0 \rho_s + \sum_{i=1}^j \Delta\sigma_c(t_i) A_0 (1 - \rho_s) = 0,$$

$$N(t_i) = N_c(t_i) + N_s(t_i),$$

$$\sum_{i=1}^j \Delta\varepsilon_c(t_i)$$

$$= \left(\sigma_c(t_0) J(t_j, t_0) + \sum_{i=1}^j (\Delta\sigma_c(t_i) J(t_j, t_i)) + \varepsilon_{sh}(t_j, t_0) \right)$$

$$- \varepsilon_c(t_0), \quad (9)$$

where $\sum_{i=1}^j \Delta\varepsilon_s(t_i) = \sum_{i=1}^j \Delta\sigma_s(t_i)/E_s$ denotes the strain increment accumulation and the $J(t_j, t_0)$ represents the creep compliance.

Then, the following equations can be obtained:

$$\sum_{i=1}^j \Delta\varepsilon_s(t_i) = \sum_{i=1}^j \Delta\varepsilon_c(t_i), \quad (10)$$

$$E_s \left(\sigma_c(x, t_0) J(t_j, t_0) + \Delta\sigma_c(x, t_0) J(t_j, t_0) \right.$$

$$\left. + \sum_{i=1}^{j-1} \Delta\sigma_c(x, t_i) J(t_j, t_i) - \varepsilon_c(x, t_0) \right) A_0 \rho_s \quad (11)$$

$$+ \left(\Delta\sigma_c(x, t_j) + \sum_{i=1}^{j-1} \Delta\sigma_c(x, t_i) \right) A_0 (1 - \rho_s) = 0,$$

$$\varepsilon_c(x, t_0) = \frac{\sigma_c(x, t_0)}{E_c(t_0)}. \quad (12)$$

Substituting (10) and (11) into (12), the stress increment of concrete in time t_i $\Delta\sigma_c(x, t_i)$ can be expressed as

$$\Delta\sigma_c(x, t_i)$$

$$= - \left(\rho_s \sigma_c(x, t_0) (E_s J(t_j, t_0) - m_e(t_0)) \right.$$

$$+ E_s \rho_s \left(\sum_{i=1}^{j-1} \Delta\sigma_c(x, t_i) J(t_j, t_i) \right) \quad (13)$$

$$\left. + \sum_{i=1}^{j-1} \Delta\sigma_c(x, t_i) (1 - \rho_s) \right)$$

$$\times (1 + (E_s J(t_j, t_j) - 1) \rho_s)^{-1}.$$

The stress increment of concrete in time t_1 is expressed as

$$\Delta\sigma_c(x, t_1) = - \frac{\rho_s \sigma_c(x, t_0) (E_s J(t_1, t_0) - m_e(t_0))}{1 + (E_s J(t_1, t_1) - 1) \rho_s}. \quad (14)$$

Substituting (14) into (5), the stress increment of reinforcement in time t_1 is expressed as

$$\Delta\sigma_s(x, t_1) = \frac{(1 - \rho_s) \sigma_c(x, t_0) (E_s J(t_1, t_0) - m_e(t_0))}{1 + (E_s J(t_1, t_1) - 1) \rho_s}. \quad (15)$$

In (14) and (15), stress increments of concrete are always negative and the stress increments of reinforcement are always positive in the long-term process. Consequently, under the long-term constant load, the force acted on the concrete is decreasing while the force acted on the reinforcement is increasing. In other words, the internal force is transferred from concrete to reinforcement bars due to the creep effect.

3.4. Case 4: Effect of Reinforcement on Ultimate Tensile Strain of Concrete. Effect of reinforcement on ultimate tensile strain for concrete structure is a controversial issue. Some researchers indicate that there is no effect of reinforcement on ultimate tensile value, but some others indicate that the existence of reinforcement improves the ultimate tensile value for concrete structure [7].

The relationship between reinforcement and the ultimate tensile strain of concrete structure can be illustrated by the empirical formula [7]:

$$\varepsilon_{pa} = 0.5R_f \left(1 + \frac{p}{d} \right) \times 10^{-4}, \quad (16)$$

where ε_{pa} denotes the ultimate tensile strain of concrete structure; R_f is the tensile strength of concrete (MPa); $p = 100\mu$; μ represents the reinforcement ratio; d means the diameter of the reinforcement bar (cm).

According to (16), the ultimate tensile strain of Specimen 4 is equal to 141×10^{-6} . Besides, ultimate tensile value of Specimen 4 is 135.7×10^{-6} (Figure 7(d)). Therefore, a reasonable amount of agreement was achieved between the experimental results and the calculation values. Moreover,

Figure 7(d) illustrates that the ultimate tensile strain value of RC specimen is approximately 105% higher than that of the plain concrete. The reason for this phenomenon may be that tiny cracks can enhance the specimen strain capacity before the occurrence of the first through crack, with the assumption that the formation of tiny cracks is initiated by a crack forming zone developing around the reinforcement bars [23].

4. Conclusions

A modified TSTM has been developed to investigate the early-age cracking behavior of concrete and RC. Based on the experimental results, effects of concrete placing temperature, cooling rate, and reinforcement on concrete cracking were quantitatively analyzed. The following conclusions are drawn from this experimental study.

- (1) Case 1 showed that the lower cooling rate can reduce the probability of concrete cracking and postpone the concrete cracking, considering that the cracking temperature and the crack reserve of the two tests (Test 1 and Test 2) are (26.11°C, 17.29°C) and (1.95%, 30.55%), respectively.
- (2) Case 2 showed that concrete with lower placing temperature has a lower probability of concrete cracking. In detail, the cracking temperature of Test 3 is 13.9°C lower than that of Test 1, and the stress reserve of Test 3 is about 31.24% higher than that of Test 1.
- (3) Case 3 showed that reinforcement bars can postpone the occurrence of the first major crack appearance. Compared with the plain concrete, the cracking moment of RC was delayed about 108 hours; the stress reserve was improved by 25.74%, and the cracking temperature was declined by 21.45°C (in these experimental conditions). Besides, reinforcement can increase the maximum tensile strength of RC specimen by nearly 30% in this experiment. Moreover, considering the axial tension specimen under long-term load, the internal force could transfer from concrete to reinforcement bars due to the creep effect.
- (4) Both the calculation and experiment of Case 4 prove that reinforcement can enhance the ultimate tensile strain of the structure. Moreover, the ultimate tensile strain value of RC specimen is approximately 105% higher than that of plain concrete in the paper.

Conflict of Interests

The authors declare that there is no conflict of interests regarding the publication of this paper.

Acknowledgments

This study was part of a research project supported by China Three Gorges Corporation (Grant no. TGC-2012746379) and Hekoucun Reservoir Concrete Engineering Projects (Grant no. HKCSK-KY-01). The authors would also like to express

their gratitude for the financial support that has made the study possible. The authors would like to thank Dr. Chen Yanyu from Stony Brook University for revising the language of this paper.

References

- [1] ACI Committee 116R, *Cement and Concrete Terminology*, Concrete International, 2005.
- [2] M. Briffaut, F. Benboudjema, J. Torrenti, and G. Nahas, "Effects of early-age thermal behaviour on damage risks in massive concrete structures," *European Journal of Environmental and Civil Engineering*, vol. 16, no. 5, pp. 589–605, 2012.
- [3] M. Azenha, R. Faria, and D. Ferreira, "Identification of early-age concrete temperatures and strains: monitoring and numerical simulation," *Cement and Concrete Composites*, vol. 31, no. 6, pp. 369–378, 2009.
- [4] K. H. Bayagoob, J. Noorzaeei, A. A. Abdulrazeg et al., "Coupled thermal and structural analysis of roller compacted concrete arch dam by three-dimensional finite element method," *Structural Engineering and Mechanics*, vol. 36, no. 4, pp. 401–419, 2010.
- [5] ACI Committee 207, "Cooling and insulating systems for mass concrete," *Concrete International*, vol. 2, no. 5, pp. 45–64, 1980.
- [6] P. K. Mehta and J. M. Monteiro, *Concrete: Microstructure, Properties and Materials*, McGraw Hill, New York, NY, USA, 2005.
- [7] B. F. Zhu, *Thermal Stressed and Temperature Control of Mass Concrete*, China Electric Power Press, Beijing, China, 2003.
- [8] W. Srisoros, H. Nakamura, M. Kunieda, and Y. Ishikawa, "Analysis of crack propagation due to thermal stress in concrete considering solidified constitutive model," *Journal of Advanced Concrete Technology*, vol. 5, no. 1, pp. 99–112, 2007.
- [9] S. R. Sabbagh-Yazdi, F. M. Wegian, and E. Ghorbani, "Investigation of the embedded cooling pipe system effects on thermal stresses of the mass concrete structures using two phase finite element modeling," *Kuwait Journal of Science and Engineering*, vol. 35, no. 2, pp. 1–18, 2008.
- [10] S. Wu, D. Huang, F. Lin, H. Zhao, and P. Wang, "Estimation of cracking risk of concrete at early age based on thermal stress analysis," *Journal of Thermal Analysis and Calorimetry*, vol. 105, no. 1, pp. 171–186, 2011.
- [11] F. Sheibany and M. Ghaemian, "Effects of environmental action on thermal stress analysis of Karaj concrete arch dam," *Journal of Engineering Mechanics*, vol. 132, no. 5, pp. 532–544, 2006.
- [12] F. Lin, X. Song, X. Gu, B. Peng, and L. Yang, "Cracking analysis of massive concrete walls with cracking control techniques," *Construction and Building Materials*, vol. 31, pp. 12–21, 2012.
- [13] C. X. Qian and G. B. Gao, "Reduction of interior temperature of mass concrete using suspension of phase change materials as cooling fluid," *Construction and Building Materials*, vol. 26, no. 1, pp. 527–531, 2012.
- [14] Y. M. Zhu, J. R. He, and Y. J. Liu, "Temperature control and crack prevention of Long-tan High RCC Gravity Dam with different concrete placement temperatures in summer," *Water Power*, no. 11, pp. 32–36, 2002.
- [15] A. I. H. Malkawi, S. A. Mutasher, and T. J. Qiu, "Thermal-structural modeling and temperature control of roller compacted concrete gravity dam," *Journal of Performance of Constructed Facilities*, vol. 17, no. 4, pp. 177–187, 2003.

- [16] J. Yang, Y. Lee, and J. Kim, "Heat transfer coefficient in flow convection of pipe-cooling system in massive concrete," *Journal of Advanced Concrete Technology*, vol. 9, no. 1, pp. 103–114, 2011.
- [17] J. Yang, Y. Hu, Z. Zuo, F. Jin, and Q. Li, "Thermal analysis of mass concrete embedded with double-layer staggered heterogeneous cooling water pipes," *Applied Thermal Engineering*, vol. 35, no. 1, pp. 145–156, 2012.
- [18] J. Z. Pan, "Temperature reinforcement of hydraulic reinforced concrete structure," *Water Resources and Hydropower Engineering*, no. 2, pp. 29–39, 1978.
- [19] W. Q. Fu and S. F. Han, "The prevention and control of crack in concrete structures," *Concrete*, no. 5, pp. 3–14, 2003.
- [20] M. Briffaut, F. Benboudjema, J. M. Torrenti, and G. Nahas, "A thermal active restrained shrinkage ring test to study the early age concrete behaviour of massive structures," *Cement and Concrete Research*, vol. 41, no. 1, pp. 56–63, 2011.
- [21] M. Sule, *Effect of reinforcement on early-age cracking in high strength concrete [Ph.D. thesis]*, Delft University of Technology, Delft, The Netherlands, 2003.
- [22] R. Springenschmid, R. Breitenbacher, and M. Mangold, "Development of the crack frame and the temperature-stress testing machine," in *Thermal Crack in Concrete at Early Age*, RILEM, pp. 137–144, E&FN Spon, London, UK, 1994.
- [23] R. Zhang, N. Shi, and D. Huang, "Influence of initial curing temperature on the long-term strength of concrete," *Magazine of Concrete Research*, vol. 65, no. 6, pp. 358–364, 2013.
- [24] B. Chen, Y. Cai, J. Ding et al., "Comprehensive evaluation of crack resistance for dam concrete based on temperature stress testing machine," in *Proceedings of International Conference on Crack Path*, Vicenza, Italy, 2009.
- [25] Z. P. Bazant, "Nonlinear creep buckling of reinforced concrete columns," *Journal of Structural Engineering*, vol. 106, no. 11, pp. 653–661, 1980.



Hindawi

Submit your manuscripts at
<http://www.hindawi.com>

